RSC Advances

ROYAL SOCIETY OF CHEMISTRY

www.rsc.org/advances

Effects of a New Crystal Structure of Poly(Vinylidene Fluoride-Hexafluoropropylene)/Poly(Mathyl Methacrylate) Blend Films on Discharge Efficiency

Guirong Peng[1], Xiaojia Zhao, Zaiji Zhan, Shengzong Ci, Qian Wang, Yanjuan Liang, Mingliang Zhao

(State Key Laboratory of Metastable Materials Science and Technology, Yanshan University, Qinhuangdao, 066004, P. R. China)

Abstract： A series of PMMA/poly(vinylidene fluoride-hexafluoropropylene) [P(VDF-HFP)] blend films were prepared with solution blending process to improve discharge efficiency. The properties of PMMA/ P(VDF-HFP) blend films were carefully studied. The results show that the crystallinity, the dielectric constant and the loss of the polymer blend films decreased with the increase of PMMA content XRD results demonstrate the existence of γ-2b phase. The melting points of polymer blends were increased with increasing PMMA, which is considered resulting from the phase transition of the P(VDF-HFP) crystals from α to γ-2b. The energy loss of P(VDF-HFP) reduced significantly with the addition of PMMA. The optimized blend film is the samples with 10% PMMA. The discharge efficiency of the optimized blend films was above 80% in 300MV/m. The increase in discharge efficiency is considered resulting mainly from the formation of gamma crystal.

Key words: polymer blends; crystal structure; γ-2b crystal, discharge efficiency; fluoropolymers

Introduction

Poly(vinylidene fluoride) (PVDF) and its copolymers such as those with chlorotrifluoroethylene [P(VDF-CTFE)], hexafluoropropylene [P(VDF-HFP)], and trifluoroethylene [P(VDF-TrFE)], are potential dielectric materials for a broad range of applications such as grid leveling, pulsed lasers, and electric or hybrid vehicles[1]. These ferroelectric polymers exhibit larger energy density than the widely used capacitor polymeric films, such as biaxially oriented-polypropylene (BOPP). Compared to BOPP that presents an energy density of 4 J/cm^3 at 600MV/m and a low dielectric constant of 2.2 at 1kHz, uniaxially copolymer P(VDF-CTFE) [2] possesses a high dielectric constant of 13 at 1kHz and an energy density of 25J/cm^3 at a field of 620MV/m, copolymer P(VDF-HFP) [3] (4.5 mol%HFP) displays an energy density of 25 J/cm^3 at a field of 700 MV/m, P(VDF-TrF-CTFE) [4] (65.6/26.7/7.7 mol%) which dielectric constant is above 60, exhibit an energy density of 13 J/cm^3 at 500MV/m and a discharge efficiency is about 60% at a field of 300 MV/m. However, there are still some challenges that need to be attempted before these polymers commercially used. One of the most critical issues is discharge efficiency of these ferroelectric polymers.

PVDF is a semi-crystalline polymer with about 50% crystallinity and possesses good mechanical properties, chemical resistance, electric resistance, and processability. PVDF exists in at least five crystalline forms [α(II), β(I), γ(III), δ(IV), ε(Ⅴ)][5-8]. Recently, a new crystalline variety

[1] corresponding Author: College of materials Science & Engineering, Yanshan University, Qinhuangdao 066004, P.R. China, email: gr8599@aliyun.com ; Tel(o): 86-0335-8074631; Fax:86-0335-8074545

(γ-2b) of PVDF was reported by Maja Remskar[9]. The main chain conformations of α, β, γ phases are TGTG, TTTT and TTGTTG respectively. Melting temperature (T_m) varies depending on their crystalline structure. The glass transition temperature (T_g) of PVDF is below -37°C, demonstrating that PVDF is rubbery at ambient temperature. The α-phase is non-polar, which is obtained for PVDF and its copolymer under usual melt crystallization[10]. Rinaldo Gregorio, Jr.[11]reported that β phase formed exclusively when PVDF crystallized from solution at the temperature lower than 70°C, regardless of the solvent used, as long as it is a good solvent for this polymer. The γ phase forms via the melt or anneals at temperature close to T_m of α phase. The polar β crystal possesses a large energy loss for its spontaneous polarization and hysteresis of ferroelectric switching[12].

Many researchers have prepared some copolymers such as P(VDF-CTFE), P(VDF-TFE), P(VDF-TrFE) and P(VDF-CTFE- TrFE) to tailor the crystallization of polar β-phase for improving discharge efficiency of the capacitor films. But the copolymer is very expensive. Another way to tailor the crystallization of polar β-phase is to blend with other polymers. A kind of usually used polymer is poly(methyl methacrylate) (PMMA). By melt blending or solution blending, polymer alloy of PMMA/PVDF can be prepared. In laboratory, solution blending is used mostly for its simplicity in operation and equipments. In most investigations, PVDF is considered compatible with PMMA. Wang and Nishi[13-14] have reported that semicrystalline PVDF is compatible with amorphous poly(methyl methacrylate) (PMMA) in molten state. Recently, Zhang[15] have reported that addition of PMMA into PVDF via solution blending and quenched process, the crystallinity and crystal size of PVDF decreased. As a result, energy loss decreased accordingly. Li[16, 23] have investigated ferroelectric phase diagram of P(VDF-TrFE)/PMMA. Ferroelectric β-phase were observed when the blend films were melted, ice quenched, subsequently annealed close to melting temperature of α phase. Meanwhile, the crystallinity, the remnant polarization and the roughness of blend films decreased with increasing PMMA content.

In brief, most researches consider that the PMMA can increase the defects and decrease the crystal size of β-phase, and in consequence compress the ferro-electricity of β-PVDF and increase discharge efficiency. However, in our work we found that PMMA could facilitate the formation of new crystal variety (γ-2b) of P(VDF-HFP), which is considered contribute more to the improvement of discharge efficiency. In this paper, effects of PMMA on transition of crystalline structure, degree of crystallinity and molecular mobility of P(VDF-HFP)/PMMA blend films are investigated, and then the influence of crystalline structure on discharge efficiency was investigated via D-E loops.

Experimental

Material

P(VDF-HFP) (Kynar Flex 2751-00) in powders was purchased from Arkema corporation, France. PMMA(CM-207) pellets (Mn=38406g/mol, Mw=72777g/mol, Mw/Mn=1.9) were purchased from Chi Mei corporation, Taiwan. N, N-dimethylformamide (DMF) is AR grade from Tianjin Reagents Co. Ltd.

Process of films preparation

P(VDF-HFP) and PMMA were dissolved in DMF to make polymer solutions with the DMF concentration of 90 wt%. The weight ratio of P(VDF-HFP) to PMMA is 100:0, 95:5, 90:10 and

70:30 respectively. The blend solutions were agitated magnetically for 6h, ultrasonic agitated for 30min, and casted onto glass sheet followed by drying at 120 °C, subsequently at 160 °C under vaccum for 8h. The thickness of the films is about 30±5 μm.

Characterization

FTIR spectroscopy was measured with an IR spectrometer (E55+FRA106) at a 0.5 cm^{-1} resolution and in the 600-4000 cm^{-1} wave number range in attenuated total reflection (FTIR-ART). X-ray diffraction (XRD) measurements were performed on an X-ray Diffractometer (M03XHF22, MACScience corporation, Japan) with Cu K_α radiation (λ=0.154 nm), a scanning range of 2θ=10-55°, and a scanning rate of 5°/min. Differential scanning calorimetry (DSC) analysis was conducted on a Netzsch STA449C (Netzsch Corp., Germany) under Ar protection to measure the melting temperature and crystallinity at a heating rate of 5℃/min.

Dielectric constant and loss were measured at different frequencies range of 100Hz to 1MHz and temperature range 0-150 °C and at 1 V on Broad frequency dielectric spectrometer (Concept 80, Germany). Relative permittivity ε is calculated by the following formula: $\varepsilon = \frac{t \times C_p}{A \times \varepsilon_0} = \frac{t \times C_p}{\pi (d/2)^2 \times \varepsilon_0}$ where, ε is relative permittivity, ε_0 is permittivity of free space (8.854×10^{-12}F/m), Cp is the capacitance, t is material thickness, A is the area of the electrode, and d is the diameter of the electrode. Three points for each sample are measured with micrometer, the accuracy is 0.001mm, and the max range of the thickness error of the samples is ±1 μm. For most samples, the three thickness data of each sample is same. Our sample for each composition is uniform in thickness.

The electric D-E loops were measured with a modified Sawyer–Tower circuit. The samples were subjected to a unipolar wave, with frequency of 10 Hz. The D-E loops are presented according to the data from the first cycles.

Results and Discussion

3.1 Structure characterization of PMMA/PVDF blends

FTIR-ART spectra were used to investigate the crystalline phases of the PVDF-HFP/PMMA composite films with various PMMA content, the results are shown in Figure 1. The peak at 879cm^{-1} were attributed to the amorphous phase of PVDF-HFP and could not be used to identify any of crystalline phases[15].The absorption peaks at 1724.32, 1726.22, 1728.2, and 1730.01 cm^{-1} were ascribed to the stretching of carbonyl groups, which suggest the existence of PMMA in the blends. Usually, the asymmetry carbonyl bonds absorptions are resulted from the coexisted of dissociated carbonyl and hydrogen bonded carbonyl. The dissociated carbonyl bonds usually locate at 1733 cm^{-1}. When hydrogen bonds are formed, the absorption peak will shift to red. The red-shift wave-number increases with the hydrogen bond strength. For the blends of PMMA/PVDF, the absorptions of carbonyl groups shifted to higher wave-numbers compared with pure PMMA, but the absorption peaks are still asymmetry. The asymmetry carbonyl absorptions are enlarged and fitted with gauss function, as shown in Figure 2. It can be seen that the asymmetry peak can be split to two peaks. If the dissociated carbonyl absorption is set at a fixed position, then the position of hydrogen bonded carbonyl shift from 1719.5 cm^{-1} of pure PMMA to

1721.5 cm^{-1} of the mixture, which means that the hydrogen bonds might change its strength. All of these indicated that the hydrogen bonds within PMMA might change to that between PMMA and PVDF.

The absorption peaks at 613cm^{-1}, 763cm^{-1}, 1072cm^{-1} and 1402cm^{-1} were assigned to α phase of PVDF-HFP. The peaks at 840cm^{-1} and 1431cm^{-1} were characteristic of β phase[17,18] which are multiplied with the absorption peaks of PMMA at the wave-number. The bonds at 813cm^{-1}, 834cm^{-1} and 1231cm^{-1} were associated with γ phase of PVDF-HFP[19], which are affected by the absorption of PMMA. From the Figure, after blending with PMMA, more absorptions of PMMA were revealed with the increase in PMMA percent, and the absorptions of PVDF show no significantly change, but it seemed that alpha and gamma phases are the major.

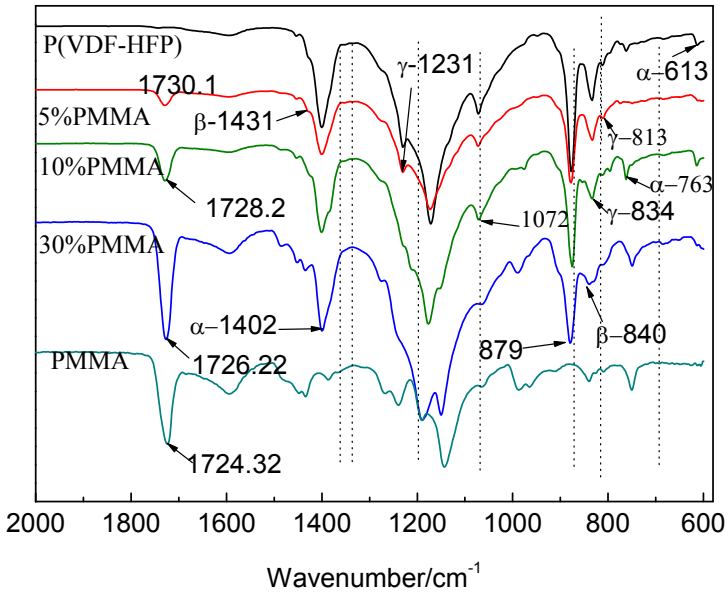

Figure 1 FTIR spectra of PVDF-HFP/PMMA thin films with various PMMA content

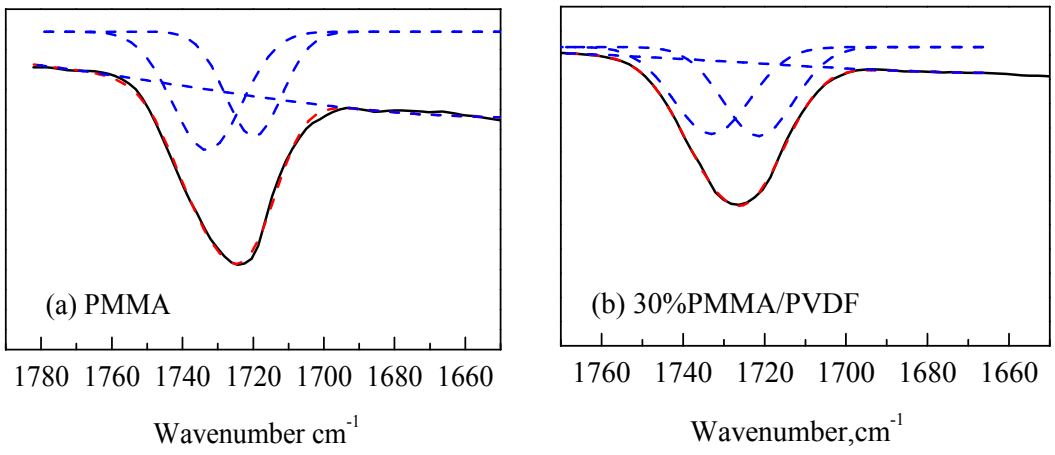

Figure 2 Fitting results of carbonyl absorptions with gauss function for pure PMMA (a) and 30%PMMA/PVDF (b)

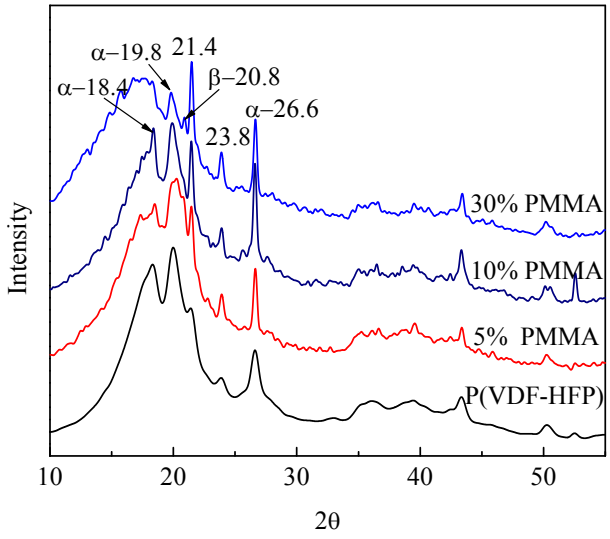

Figure 3 X-ray diffraction patterns of PVDF-HFP/PMMA blends with various PMMA content

X-ray diffraction patterns of PVDF-HFP copolymer and PVDF-HFP/PMMA blends were shown in Figure 3. Three peaks at 2θ=18.4, 19.8 and 26.6 were observed in PVDF-HFP copolymer and PVDF-HFP/PMMA blends thin films, which corresponded to the reflections of α(020), (110) and (021) respectively. The peak at 2θ=20.8 was observed in blends as single peak or shoulder peak, which is planes (110) and (200) of β phase[15]. In addition, two peaks at 2θ=21.4 and 23.8 were observed in all thin films, which corresponded to the reflections of γ-2b (022) and (032) respectively according to the work of Maja Remskar [9]. Compared with the peak of α crystal, the intensity at 2θ=21.4 and 23.8 was increased significantly with the increase of PMMA content. This showed that addition of PMMA promoted the formation of γ-2b phase under the heat treatment condition.

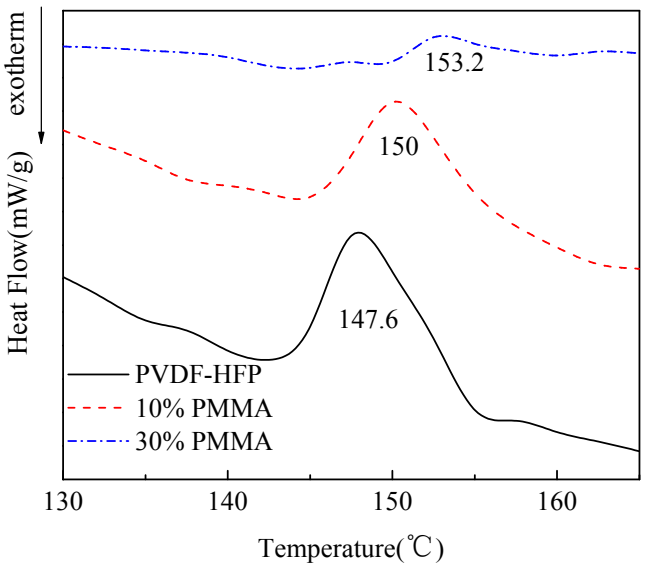

Figure 4 DSC curves of P(VDF-HFP) blends with various PMMA content

The DSC heating thermograms of the PVDF-HFP film and P(VDF-HFP)/PMMA blend films

are shown in Figure 4. When PMMA content is increased from 0 to 30%, the melting temperature rises slightly from 147.6 °C to 153.2 °C. This rising should be resulted from the formation of γ-2b phase in the polymer. The melting temperature of γ crystal is higher than that of α and β phases[20]. The crystallinity of the polymer decreased obviously when the content of PMMA increased to 30%. This change might be induced by the dilution effect of PMMA.

3.2 Dielectric properties of PMMA/PVDF blends

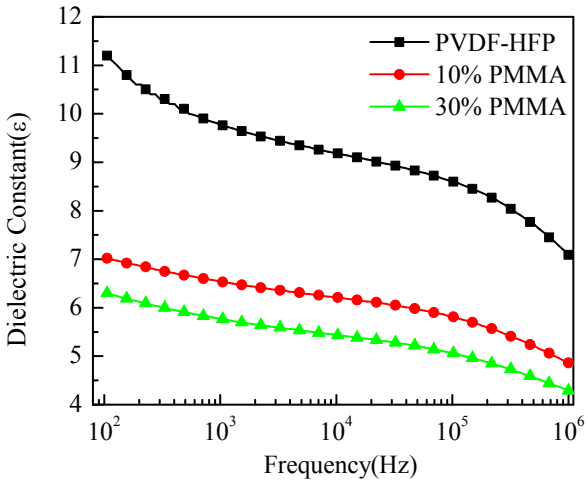

Figure 5 Dielectric constant of PMMA/P(VDF-HFP) with different PMMA content at room temperature (about 20°C)

Figure 5 shows the variation of dielectric constant of P(VDF-HFP) /PMMA with PMMA percent. As shown in the Figure, the dielectric constant decreased with the increase of PMMA content, especially in high frequency ($> 10^5$Hz). It is mostly because the flip of polar chain segment lags behind the high frequency. Compared to blend films, the dielectric constant of P(VDF-HFP) film sharply decreased with the increase of frequency, indicating the frequency dependence of P(VDF-HFP) film is stronger than the blend films. In addition, compared to P(VDF-HFP), the dielectric constant of the blend films decreased due to the dilution effect of amorphous PMMA. From the structure, the γ phase can show bigger polarity than α crystal, and could benefit to the increase of dielectric constant, but the experiment results shows obvious decrease, which means that γ phase can not compensate for the loss in dielectric constant resulting from the addition of PMMA.

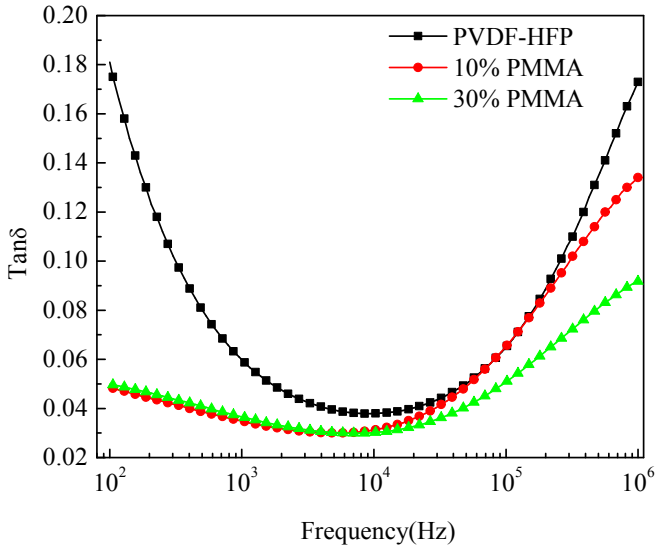

Figure 6 Dielectric loss vs frequency of P(VDF-HFP)/PMMA films with different PMMA content at room temperature (about 20°C)

Figure 6 showed the variation of Tanδ of P(VDF-HFP)/PMMA with PMMA content. Dielectric loss of all thin films at about 20°C changed in V-shape with frequencies. For blend films, dielectric loss is significantly lower than P(VDF-HFP) at lower frequency, and was slightly decreased at higher frequencies. The dielectric loss mainly comes from conductance loss ($<10^4$) and polarization loss (10^4-10^6). The conductance loss decreases with increasing frequency at low frequency, and polarization loss is negligible. Therefore, the dielectric loss of blend film under low frequency would reduce with increasing frequency, but gradually the relaxation polarization couldn't keep up with the change of the electric field frequency at high frequency, and hysteresis phenomenon began to appear, thus polarization loss produced. The rising speed of polarization loss is much higher than the reduced speed of conductance loss. So the dielectric loss increased with frequency at higher frequency range [21]. When PMMA content is 30%, the dielectric loss significantly decreased due to dipole moments flipped difficultly. The reason is that the interactions of C=O in PMMA and CH_2 in PVDF hinder the movement of the chains and decreased the flip of dipole. Thus, dielectric loss of blend films decreased.

The temperature dependence of dielectric constant for P(VDF-HFP) and P(VDF-HFP)/ PMMA films were measured at 1.05kHz. As shown in Figure 7a, for P(VDF-HFP), the dielectric constant was sharply increased above 50 °C. The dielectric constants of all thin films increased with temperature due to an increase of the total polarization, which in the polyblend might be rising from dipoles and trapped charge carriers, occurring at the interface of crystal and amorphous phase[22].

The curves of dielectric loss against temperature at 1.05k Hz were shown in Figure 7b.The dielectric loss values of all thin films increased with temperature increasing. Compared to blends, the tanδ value of P(VDF-HFP) sharply increased with temperature. With the increase of PMMA content, the dramatic increase point of tanδ shifted to higher temperature, and became unobvious when the content of PMMA increased to 30 wt%. As shown in Figure 4, after addition of PMMA,

the melting point increased, which means more restriction to the movements of chains and segments. From another aspect, hydrogen bonding between C=O in PMMA and CH_2 in P(VDF-HFP) can be formed, which will show bigger steric hindrance for the bigger MMA groups, as a consequence, the relaxation of the chains and segments will shift to higher temperature.

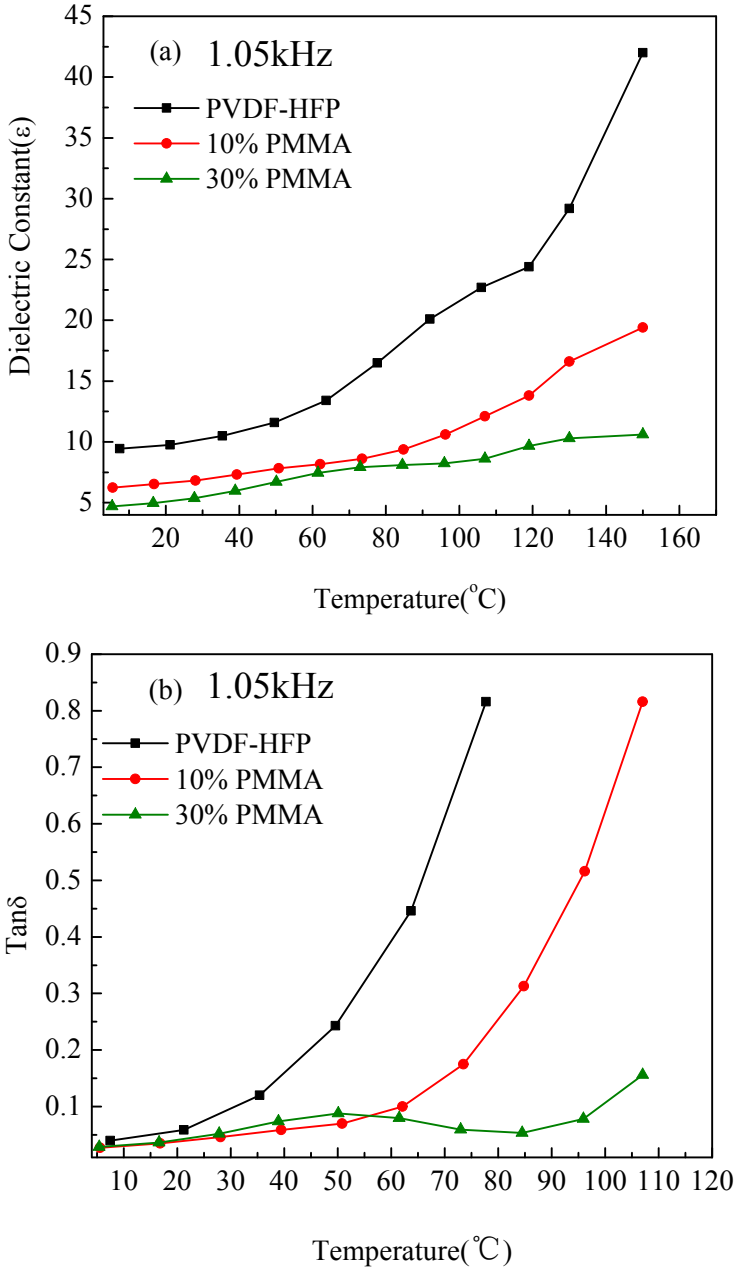

Figure 7 Temperature dependence of dielectric constant (a) and loss (b) for P(VDF-HFP)/PMMA films with different PMMA content at 1.05k Hz.

3.3 Ferroelectric property of PMMA/PVDF blends

The unipolar D-E loops of P(VDF-HFP) and P(VDF-HFP)/PMMA thin films were investigated, as shown in Figure 8. The residual polarizations of P(VDF-HFP) and 5% PMMA thin film were higher than the others, and saturation polarization can be observed. Therefore, the

energy loss was large. This was associated with the formation of β-phase. It was known that β-crystal was a ferroelectric phase. Residual polarizations and saturation polarization are the typical properties of ferroelectric phase, which are considered contributed significantly to energy loss. The residual polarization of 10% and 30% PMMA sharply decreased, and the saturation polarization did not emerge at a field of 300 MV/m. These changes should be mainly associated with γ-2b phase, which was not a ferroelectric.

By integration of the area between the D-E curves, the energy storage density and energy loss at any field can be obtained, as shown in Figure 9. It should be noticed that the max electric voltage applied in the D-E test is 10000V, which is lower than our film breakdown strengths for the film thickness is between 20 to 30 micrometers. As shown in **Table 1,** with the addition of PMMA, the breakdown strength is increased significantly, that is means the final storage strength might be much higher for the samples with PMMA more than 10 wt%.

Table 1 Breakdown strength of P(VDF-HFP) and its blend films

Sample	Shape parameter (β)	Breakdown strength E_0 (MV/m)
P(VDF-HFP)	4.43	304.57
5% PMMA	5.92	398.81
10% PMMA	6.30	540.62
30% PMMA	6.06	510.99

Note: The Breakdown strength in **Table 1** were obtained by a two-parameter Weibull distribution function: $P(E)=1-\exp[-(E/E_0)^{\beta}]$, where P(E) is the cumulative probability of failure occurring at the equal to E. The E_0 is the field strength at which there is a 63% probability for the sample to breakdown, while the shape parameter evaluates the scatter of data (＞10).

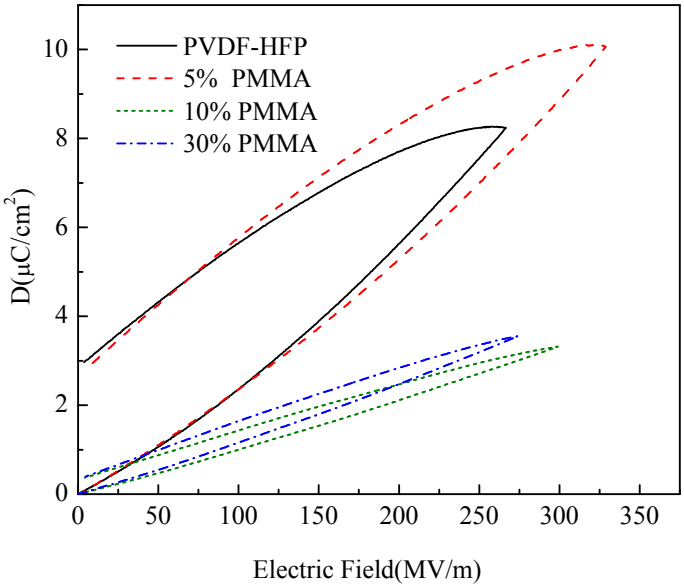

Figure 8 D–E hysteresis loops of the P(VDF-HFP)/PMMA films with different compositions under unipolar electric fields

From Figure 9, it is can be seen that the energy discharge density increased firstly and then decreased, but the energy loss decreased dramatically with the further increase of PMMA content.

For the samples with PMMA higher than 10wt%, the energy loss maintained at a low level. Therefore, the discharge efficiency calculated from the energy discharge density and energy loss showed the behavior in Figure 9 (c). For pure PVDF and that with 5wt% PMMA, the discharge efficiency decreased rapidly with electric field increasing. But for the samples with PMMA higher than 10wt%, the discharge efficiency decreased at much slower rate. The discharge efficiency increased from 45 % of pure PVDF (under 267 MV/m) to higher than 80% (under 300MV/m) for the polymer blends.

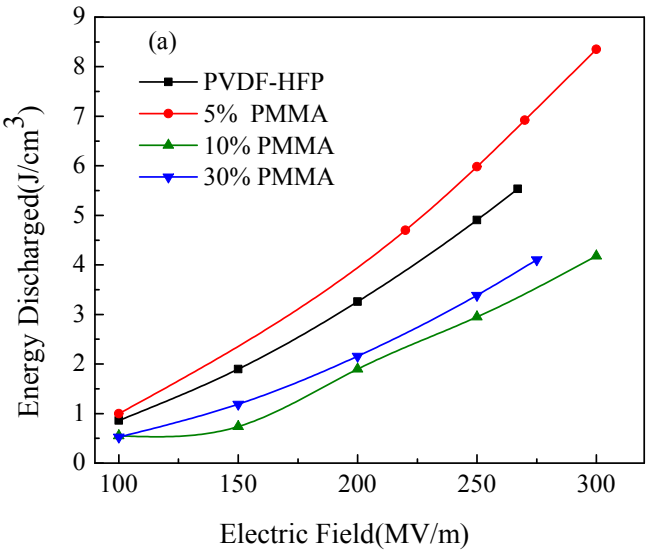

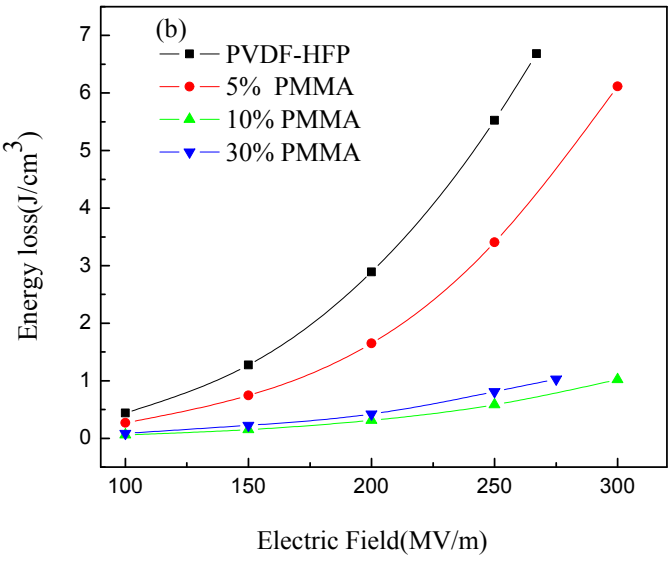

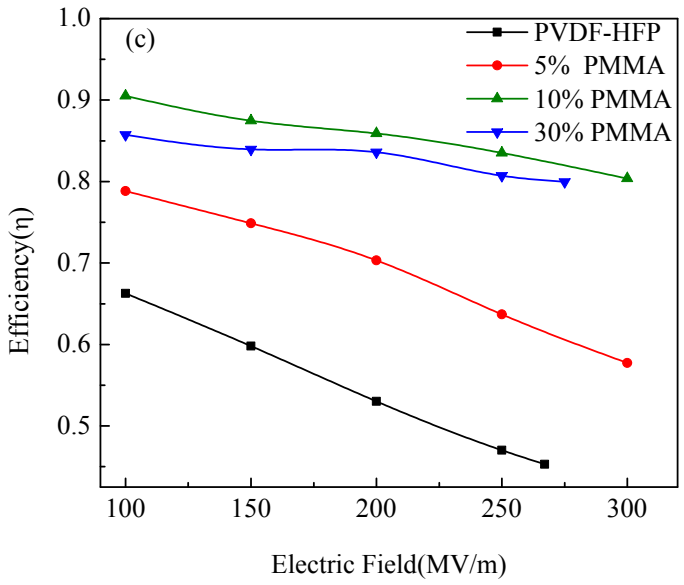

Figure 9 Energy storage (a), energy loss (b) and efficiency (c) of the PVDF-HFP/PMMA films with different compositions against electric field

The significant increase of energy discharge efficiency might be resulted from two aspects. Firstly, the addition of PMMA could result in hydrogen bonding between C=O in PMMA and CH_2 in P(VDF-HFP), which hindered the movements of chain segments. From previous results, we can see that the energy loss was shifted to higher temperature, which might be for the hindrance of hydrogen bonding to movement of PVDF segments. On one hand, the chain movement constraints from hydrogen bonds could result in the decrease of crystallinity, and consequently decreased the ferroelectric strength. On the other hand, the molecular interaction of PMMA and PVDF could orient the crystallization and promote the formation of γ-2b phase. The polarity of γ-2b phase is lower than beta phase, but higher than the alpha phase. In addition, it is not a ferroelectric, which benefit to the energy storage and can decrease the energy loss significantly. As mentioned in introduction, in most literatures, the increase of discharge efficiency is considered resulting from the decrease of beta crystallinity and increase of crystal defects. But for our results, the crystallinity of PVDF blends with 10 wt% PMMA is not decreased obviously, but the efficiency increases significantly (Figure 4). Instead, the gamma-2b signal became more obvious. Therefore, we consider that the formation of gamma crystal contributes to the increase of efficiency much more.

Conclusions

With solution blending and thermal treatment under vacuum, a series of P(VDF-HFP)/ PMMA blend films were obtained and characterized by FTIR，XRD，DSC. The results showed that crystallinity, dielectric constant and loss of P(VDF-HFP) decreased with increasing PMMA content. These changes were attributed to the dilution effect of PMMA to P(VDF-HFP). A novel γ-2b phase was observed after addition of PMMA and thermal treatment under vacuum, which

contributed to the shift of melting temperature to a higher temperature. Discharge efficiency of P(VDF-HFP) was significantly improved with the addition of PMMA to P(VDF-HFP). The blend film with 10% PMMA showed discharge efficiency of 80%, much higher than pure polymer (45%). The increase in discharge efficiency is considered resulting mainly from the formation of gamma γ crystal.

Acknowledgement

This work was funded by Natural Science Foundations of Hebei province of China (E2012203153).

References

1 V.Tomer,E.Manias,and C.A.Randall. *J.Appl.Phys.*,2011,110, 044107.

2 Xin Zhou, Baojin Chu, Bret Neese, Minren Lin and Q. M. Zhang.*IEEE Trans.Electr.lnsul.*, 2007, 14(5):1133-1138.

3 Xin Zhou,Xuanhe Zhao,higang Suo,Chen Zou,James Runt,Sheng Liu,Shihai Zhang,and Q. M. Zhang. *Appl.Phys.Lett.*, 2009, 94:16290.

4 Zhicheng Zhang and T. C. Mike Chung.*Macromolecules*, 2007, 40, 9391-9397.

5 R. Hasegawa, M. Kobayashi, M. Tadokoro. *Polym.J.*.1972, 3, 591–599.

6 J. Matsushige, T. Takemura. *J.Polym.Sci.:Polym.Phys.*.1978,16,921–934.

7 M. A.Bachmann, J. B. A. Lando. *Macromolecules*.1980,14,40–46.

8 Y.Takahashi, Y. Matsubara, H.Tadokoro. *Macromolecules*,1982,15, 334-338.

9 Maja Remskar,Ivan Iskra,Janez Jelenc,Sreco Davor Skapin,Bojana Visic,Ana Varlec and Andrej Krzan. *Soft Matter*, 2013, 9, 8647–8653.

10 T.T. Wang, J. M. Herbert and A. M. Glass, The applications of ferroelectric polymers, in *Polym.Int.*,ed. The Blackie Publishing Group, New York,1988, Vol 20, 6, 533.

11 Rinaldo Gregorio, Jr. *J.Appl.Polym.Sci.*, 2006,Vol.100, 3272–3279.

12 Wenjing Li ,Qingjie Meng,Yuansuo Zheng,Zhicheng Zhang Weiming Xia, and Zhuo Xu. *Appl .Phys. Lett.*, 2010, 96, 192905.

13 T.Nishi, T. T. Wang. *Macromolecules*, 1975, 8, 909–915.

14 T. T. Wang, T. Nishi. *Macromolecules*, 1977, 10, 421–425.

15 Qingjie Meng,Wenjing Li,Yuansuo Zheng,Zhicheng Zhang. *J.Appl.Polym.Sci.*, 2010,Vol.116, 2674–2684.

16 Mengyuan Li,Natalie Stingelin,Jasper J. Michels,Mark-Jan Spijkman,Kamal Asadi,Kirill Feldman,Paul W. M. Blom,and Dago M. de Leeuw. *Macromolecular*,2012,45,7477-7485.

17 Jung Gyu Lee,Seong Hun Kim. *Macromol. Res.*, 2011,19,1,72-78.

18 Hui-Jian Ye, Li Yang, Wen-Zhu Shao, Song-Bai Sun and Liang Zhen.*RSC Adv*., 2013, 3, 23730–23736

19 Benoit Charlot,Sebastian Gauthier, Alexandra Garraud,Philippe Combette,Alain Giani. *J.Mater Sci.:Mater. Electron*, 2011, 22:1766–1771.

20 J.Andrew, Lovinger. *Polymer*, 1980, 21, 1317-1322.

21 Kasap SO, *Principles of Electronic mMaterials and Devices*. McGraw-Hill New York: 2006.

22 G. K. Narula, P. K. C. Pillai. *J. Mater.Sci. Lett.*, 1989,9,608-611.

1 Colour graphic

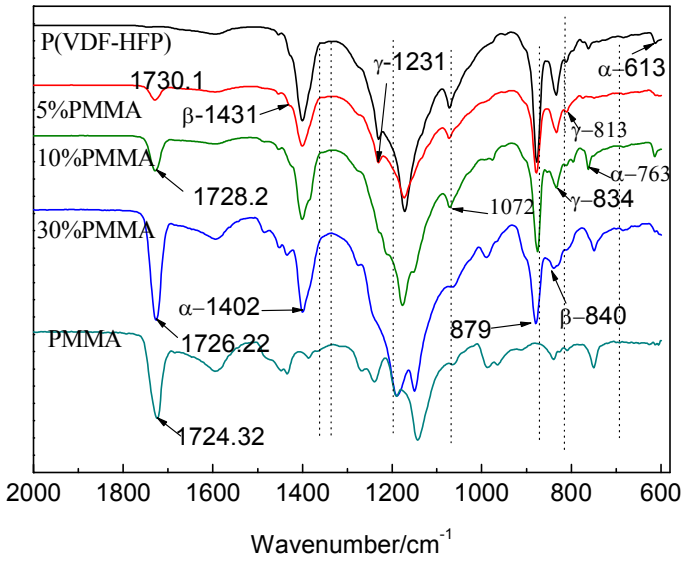

Figure 1 FTIR spectra of PVDF-HFP/PMMA thin films with various PMMA content

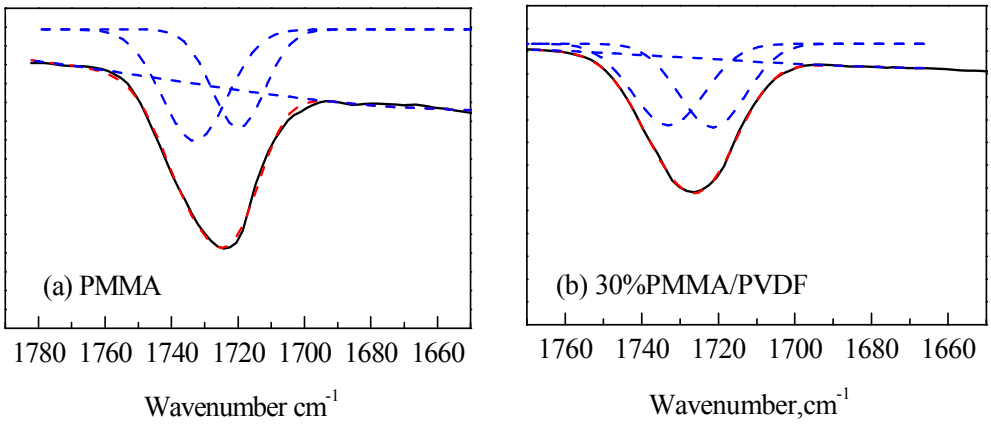

Figure 2 Fitting results of carbonyl absorptions with gauss function for pure PMMA (a) and 30%PMMA/PVDF (b)

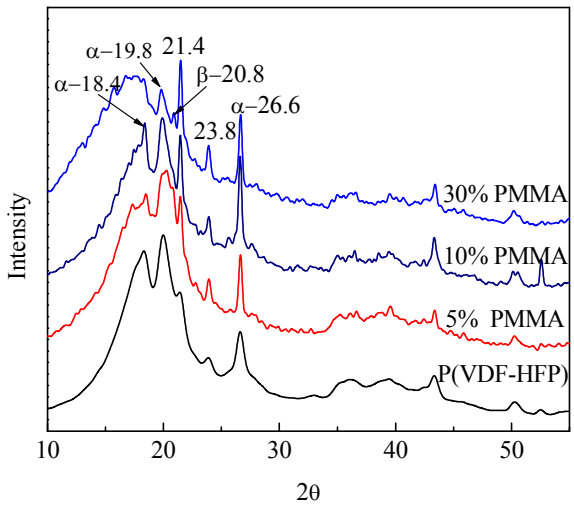

Figure 3 X-ray diffraction patterns of PVDF-HFP/PMMA blends with various PMMA content

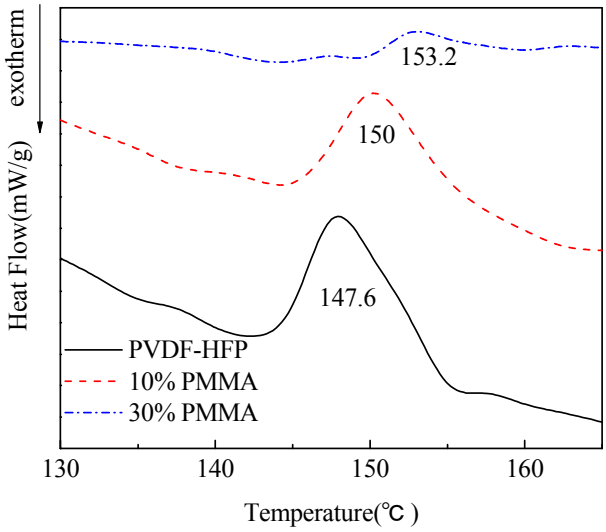

Figure 4 DSC curves of P(VDF-HFP) blends with various PMMA content

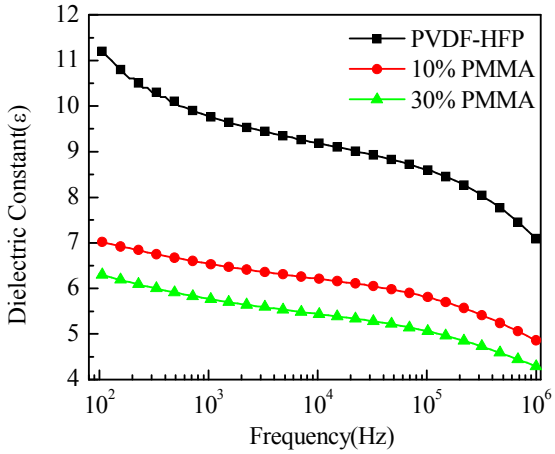

Figure 5 Dielectric constant of PMMA/P(VDF-HFP) with different PMMA content at room temperature (about 20°C)

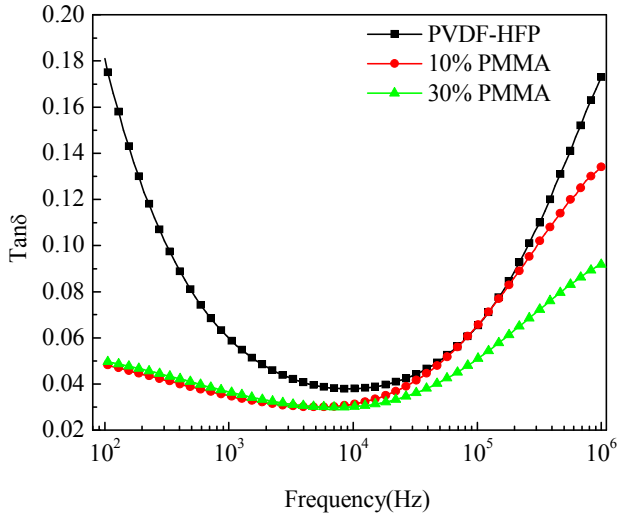

Figure 6 Dielectric loss vs frequency of P(VDF-HFP)/PMMA films with different PMMA content at room temperature (about 20°C)

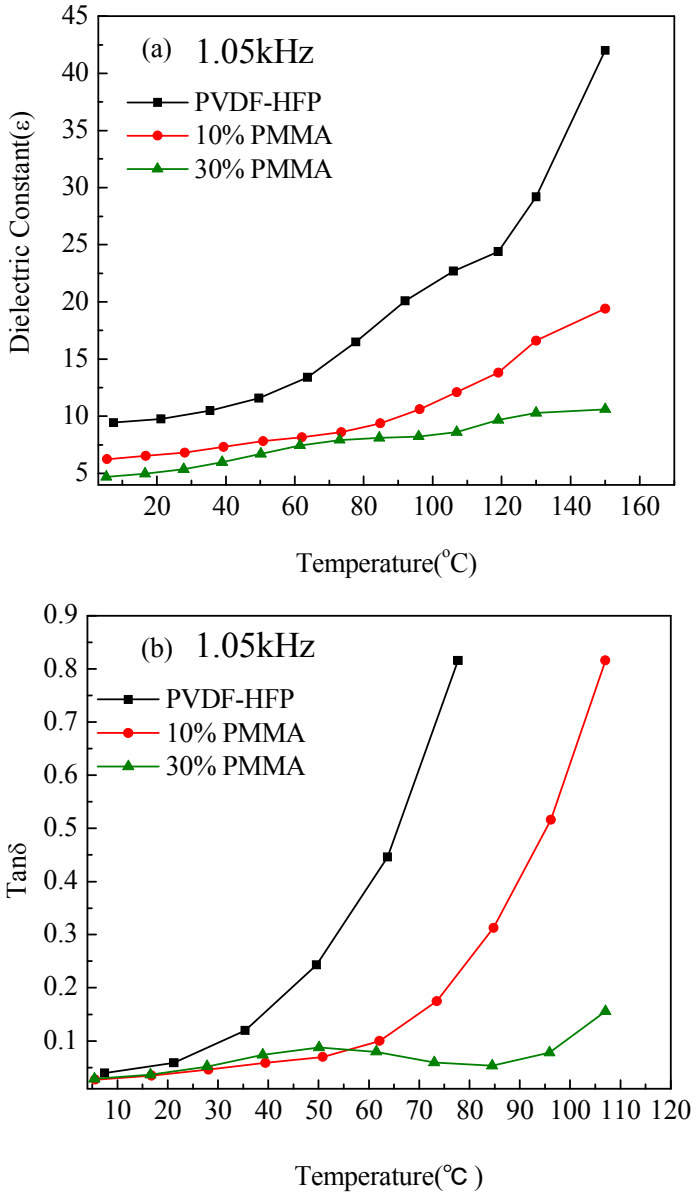

Figure 7 Temperature dependence of dielectric constant (a) and loss (b) for P(VDF-HFP)/PMMA films with different PMMA content at 1.05k Hz.

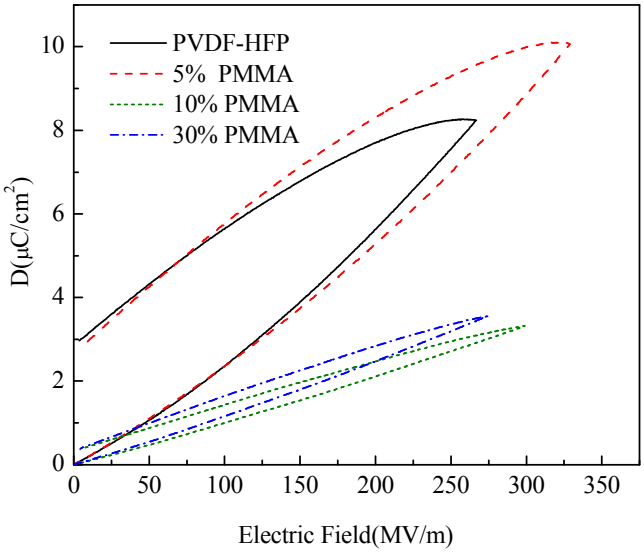

Figure 8 D–E hysteresis loops of the P(VDF-HFP)/PMMA films with different compositions under unipolar electric fields.

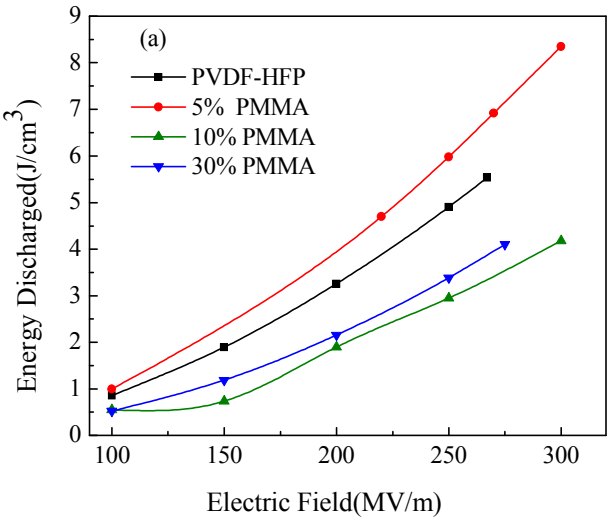

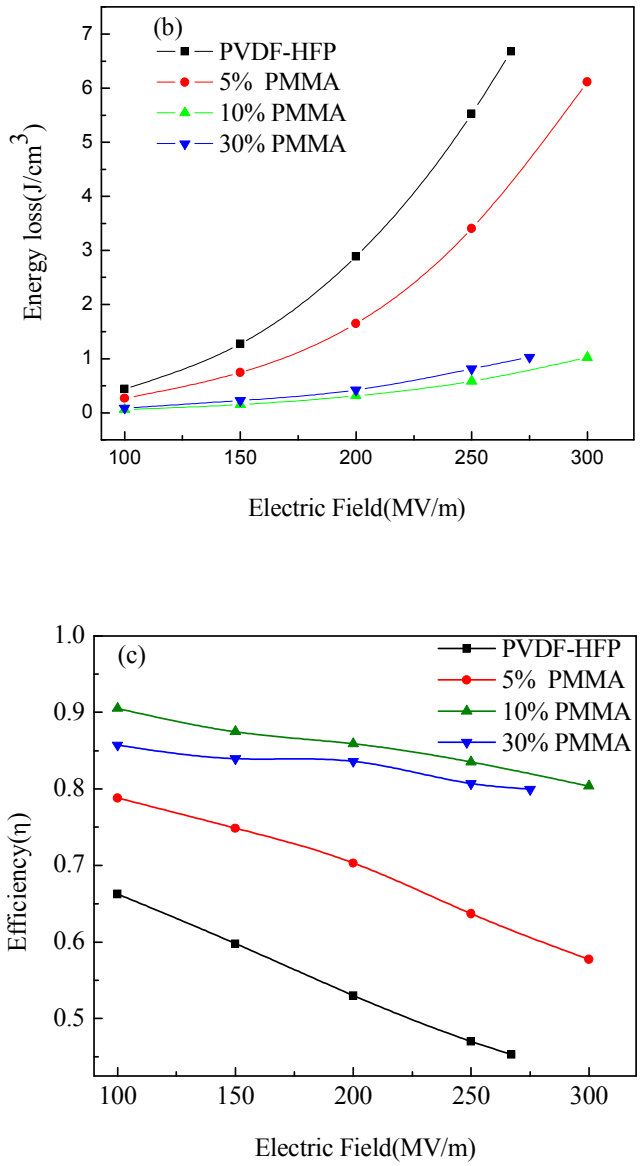

Figure 9 Energy storage (a), energy loss (b) and efficiency (c) of the PVDF-HFP/PMMA films with different compositions against electric field.

Table 1 Breakdown strength of P(VDF-HFP) and its blend films

Sample	Shape parameter (β)	Breakdown strength E_0 (MV/m)
P(VDF-HFP)	4.43	304.57
5% PMMA	5.92	398.81
10% PMMA	6.30	540.62
30% PMMA	6.06	510.99

2 the novelty of the work

In brief, most researches consider that the PMMA can increase the defects and decrease the crystal size of β-phase, and in consequence compress the ferro-electricity of β-PVDF and increase discharge efficiency. However, in our work we found that PMMA could facilitate the formation of new crystal variety (γ-2b) of P(VDF-HFP), which is considered contribute more to the improvement of discharge efficiency.